Design, synthesis and antiviral evaluation of novel heteroarylcarbothioamide derivatives as dual inhibitors of HIV-1 Reverse transcriptase-associated RNase H and RDDP functions.

Angela Corona,[a] Valentina Onnis,[a] Alessandro Deplano,[a] Giulia Bianco,[a] Monica Demurtas,[a] Simona Distinto,[a] Yung-Chi Cheng,[b] Stefano Alcaro,[c] Francesca Esposito[a] and Enzo Tramontano[a]

[a]Dipartimento di Scienze della Vita e dell'Ambiente, Università degli Studi di Cagliari, Cittadella Universitaria di Monserrato, 09042, Cagliari, Italy;

[b]Department of Pharmacology, Yale University Medical School, New Haven, CT, USA

[c]Dipartimento di Scienze della Salute, Università "Magna Græcia" di Catanzaro, Campus "S. Venuta", Viale Europa, 88100 Catanzaro, Italy

Corresponding author:

Angela Corona Ph.D.

Department of Life and Environmental Sciences University of Cagliari

Biomedical Section, Laboratory of Molecular Virology

Cittadella Universitaria di Monserrato, SS554 -

09042 Monserrato (CA)

phone: +39 0706754535

e-mail angela.corona@unica.it

Running sentence: Pyrrolyl heteroarylcarbothioamide derivatives are new dual inhibitors of both ribonuclease H and polymerase HIV-1 RT-associated functions, a new promising resource against drug resistance

Key words: HIV-1 therapeutic agents; RT dual inhibitors; HIV-1 Ribonuclease H; heteroarylcarbothioamide.

Abstract

In the continuous effort to identify new HIV-1 inhibitors endowed with innovative mechanisms, the dual inhibition of different viral functions would provide a significant advantage against drug resistant variants. The HIV-1 reverse transcriptase (RT) associated Ribonuclease H (RNase H) is the only viral encoded enzymatic activity that still lacks an efficient inhibitor. We synthesized a library of 3,5-diamino-N-aryl-1H-pyrazole-4-carbothioamide and 4-amino-5-benzoyl-N-phenyl-2-(substituted-amino)-1H-pyrrole-3-carbothioamide derivatives and tested them against RNase H activity. We identified the pyrazolecarbothioamide derivative **A15**, able to inhibit viral replication and both RNase H and RNA-dependent DNA polymerase (RDDP) RT-associated activities in the low micromolar range. Docking simulations hypothesized its binding to two RT pockets. Site directed mutagenesis experiments showed that, with respect to wt RT, V108A substitution strongly reduced **A15** IC_{50} values (12.6 fold for RNase H inhibition and 4.7 fold for RDDP), while substitution A502F caused a 9.0 fold increase in its IC_{50} value for RNase H, not affecting the RDDP inhibition, reinforcing the hypothesis of a dual site-inhibition. Moreover, **A15** retained good inhibition potency against three non-nucleoside RT inhibitor (NNRTI) resistant enzymes, confirming a mode of action unrelated to NNRTIs and suggesting its potential as a lead compound for development of new HIV-1 RT dual inhibitors active against drug resistant viruses.

1. Introduction

Human immunodeficiency virus type 1 (HIV-1) causes a persistent infection integrating its genome into the host genome and continuously replicating, requiring a life-long treatment to maintain the viral loads under control in order to avoid the progression to AIDS (Cohen et al. 2008). High viral mutation-rate and sub-optimal treatment adherence allow the selection of viral strains resistant to the approved drugs (Gregson et al. 2016), hence entailing a continuous effort by the scientific community to identify new inhibitors, possibly targeting viral coded essential proteins with innovative mechanisms.

HIV-1 Reverse Transcriptase (RT) is a key multifunctional enzyme which combines an RNA-dependent DNA polymerase activity (RDDP), a DNA-dependent DNA polymerase activity (DDDP) and a ribonuclease H (RNase H) function, all essential for the viral genome replication (Schatz et al. 1990). Up to now, all approved RT-targeting drugs inhibit only the polymerase activity (Menéndez-Arias, Sebastián-Martín and Álvarez 2016), while no inhibitor has been approved yet targeted at the RNase H, whose essential role played in retroviral replication makes it a very promising target for the development of antiretroviral agents (Corona, Esposito and Tramontano 2014). Small molecules shown to inhibit RNase H activity in preclinical studies can be grouped, according to their mode of action (Corona et al. 2013), into a) metal-chelating active site inhibitors, which can bear different scaffolds including N-hydroxyimides (Klumpp and Mirzadegan 2006), N'-acylhydrazones (Carcelli *et al.* 2017), pyrrolyl and quinolinonyl diketoacids (Corona *et al.* 2014a, 2016b; Costi *et al.* 2014; Cuzzucoli Crucitti *et al.* 2015) , 2-hydroxyisoquinoline-1,3-diones (Billamboz *et al.* 2008, 2010; Tang *et al.* 2017) , 3-hydroxypyrimidine-2,4-diones (Tang *et al.* 2011; Kumar *et al.* 2017a, 2017b), hydroxypyridone carboxylic acids (Kankanala *et al.* 2016) and various natural derivatives (Chung et al. 2011); b) allosteric RNase H inhibitors, which can be distinguished in i) allosteric selective RNase H inhibitors (Himmel et al. 2006); ii) p66/p51 interface inhibitors (Tintori et al. 2016) and iii) dual inhibitors of both RT associated enzyme functions (Wang et al. 2017).

This last class of compounds is of particular interest since the simultaneous inhibition of both RT activities would provide a significant advantage against drug resistant variants (Distinto et al. 2013). The allosteric dual RNase H/RDDP inhibition property has been described for scaffolds characterized by variously substituted aromatic portions bridged by a functionalized spacer containing moieties able to donate or accept hydrogen bonds, either linear or made by heterocyclic rings (Distinto et al. 2013; Meleddu et al. 2014, Meleddu et al. 2016). It has been proposed that these compounds are characterized by an innovative mechanism of action since

they could bind to two different RT allosteric pockets: the first one located in the DNA polymerase domain (partially overlapping the non-nucleoside RT inhibitor, [NNRTI] binding pocket), and the second one below the RNase H active site close to the interface between p66/p51 (Corona *et al.* 2016a).

Among the heterocycles, pyrrole and pyrazole derivatives have been previously investigated as NNRTIs (Patel and Park 2015; Liu et al. 2016). Pyrrole derivatives were firstly identified as NNRTIs within a mass screening of the Parke-Davis Pharmaceutical compound library. Since then the pyrrole moiety has been incorporated in several NNRTI series (Antonucci et al. 1995; Ding et al. 1995; Mao et al. 1998; Almerico et al. 2002). In particular, highly substituted pyrroles were proven to be active against HIV replication and considered a promising and versatile scaffold to develop anti-HIV agents (Antonucci et al. 1995). Later on pyrrole-based diketo acid derivatives were the first class of compound shown to selectively inhibit the RNase H function (Tramontano et al. 2005), interacting with highly conserved amino acidic residues within the RNase H domain (Corona et al. 2014a). Benzylpyrazole derivatives were also identified to act as NNRTIs (Mowbray et al. 2009), showing an excellent broad spectrum activity of against RT drug resistant variants (Corbau et al. 2010). Similarly, N-Arylpyrazolecarboxamide derivatives have been described as NNRTI showing *in vitro* activity against wild-type and NNRTI-resistant HIV-1 isolates species (Wildum et al. 2013). More recently, pyrazole derivatives have been reported as dual CCR5/CXCR4 HIV entry and RT inhibitors (Cox et al. 2015). Interestingly, despite their lack of HIV-1 RT-associated RDDP inhibitory activity, some N-benzylpyrazole derivatives inhibited the synthesis of early RT products (Kim et al. 2015).

Noteworthy, the potential of functionalized pyrrole and pyrazole moieties for the design and the identification of dual function RT allosteric inhibitors have not been explored yet. Hence, in the present work we synthesized a library of 1H-pyrrole-3-carbothioamide and 1H-pyrazole-4-carbothioamide derivatives and tested them on the HIV-1 RNase H activity and viral replication. The pyrazolecarbothioamide derivative **A15** was identified as the most promising compound since it was able to inhibit RNase H activity in the low micromolar range and showed to be slightly active against viral replication. Thus, this compound was also tested on the RDDP HIV1-RT activity and shown to be a new dual HIV-1 RT-associated functions inhibitor. Therefore its possible mechanism of action was investigated by means of biochemical and *in silico* studies.

2. Results and Discussion

We considered a small in-house library of 38 compounds, 18 3,5-diamino-N-aryl-1H-pyrazole-4-carbothioamide derivatives and 20 4-amino-5-benzoyl-N-phenyl-2-(substituted-amino)-1H-pyrrole-3-carbothioamide derivatives. All compounds own the described pharmacophoric requirements for RNase H/RDDP inhibition (Distinto et al. 2013; Meleddu et al. 2015), with two or three substituted aromatic rings linked by a functionalized spacer containing moieties able to donate or accept hydrogen bonds (Figure 1).

2.1 Biological activity

To identify dual inhibitors, our approach was to firstly test compounds against the RT-associated RNase H function. Results showed that 15 out of 38 tested compounds inhibited the RNase H activity with IC_{50} values ≤20 μM (Table 1 and 2).

In particular, among the pyrazole-4-carbothioamide derivatives, the diphenyl derivative **A1** showed an IC_{50} value of 98 μM (Table 1), while the introduction of a phenylacetyl substituent in R led to a consistent increase in potency (**A2**, IC_{50} value of 19 μM (Table 1). The introduction of a 4-chlorine into the phenylacetyl moiety led to compound **A5**, showing a further improved activity (IC_{50} value of 4 μM). The anti-RNase H activity was maintained by replacing the carbothioamide moiety with the carboxamide group (compound **A6**, IC_{50} 5 μM), while the introduction of a second halogen into the 4-Cl phenylacetyl (**A7**) led to a complete loss of activity. Interestingly, the introduction of substituents on the benzoyl moiety in 4-(chlorophenyl) acetyl carbothioamide derivatives was detrimental for the activity (compounds **A8**-**A14**), with the exception of **A13** (IC_{50} 21 μM), whereas the cotemporaneous presence of a 4-chlorobenzoyl moiety and a phenyl carbothioamide, led to an increase in potency (compound **A15** IC_{50} of 7 μM). Moreover the introduction a methylene spacer between the carbothioamide nitrogen and the phenyl ring (compound **A16**) or the presence of a small acyl group on pyrazole N-1 (compounds **A17**-**18**) led to a consistent loss in activity.

Among the pyrrole derivatives, 7 out of 20 compounds exhibited IC_{50} values in the low micromolar range (Table 2). Results showed that the 4-methylbenzoyl moiety in the 2-amino group led to compounds (**B1**-**B6)** showing IC_{50} values ranging form 6 to 8 μM, with the exception of 4-chlorophenylamino and of 3,4-dichlorophenylamino derivatives. The replacement of the 4-methylbenzoyl group with a 4-methoxybenzoyl was detrimental for the activity, since among compounds **B7**-**B13** only the 4-phenylamino derivative **B8** retained some RNase H inhibition properties (IC_{50} of 19 μM). Differently, in the 4-chlorobenzoyl-pyrrole series (**B14**-**B17**) the presence of 4-chlorophenylamino group did not affect RNase H potency of inhibition, since **B17** showed the same potency of inhibition observed for 4-methylphenylamino and 4-methoxyphenyl analogs **B15** and **B16** (IC_{50} values of 8-9 μM). Finally, the replacement of the aroyl moiety with a small alkylamino group (**B18**) or a

pyridylamino moiety (**B20**) was detrimental for the anti-RNase H activity in the pyrrole derivatives bearing an unsubstituted benzoyl moiety, while its replacement whit a phenyl acetyl moiety (**B19**) preserved the activity.

Next, all compounds showing IC_{50} values below 20 μM were screened for antiviral activity in cell-based assays. Results showed that the pyrazole-4-carbothioamide derivatives were not cytotoxic and that one of them, compounds **A15**, inhibited HIV-1 replication in cell based assays with an EC_{50} value of 25 μM, showing a selectivity index of 1.8 (Table 3). Differently, all tested pyrrole derivatives were cytotoxic.

Searching for dual function RT inhibitors, we then tested compound **A15** on the RT-associated RDDP activity showing that **A15** inhibited it an IC_{50} value of 17 μM (Figure S1). Hence, compound **A15** was shown to be a dual RNase H /RDDP RT inhibitor with a 2-fold higher potency for RNase H inhibition and, to acquire information useful to optimize the scaffold, we investigated its mechanism of action and binding mode.

*2.2 **A15** derivative metal chelating and dimer stability interfering properties*

To gain more insights into the **A15** mode of action we firstly asked whether it could bind to the RT active site chelating the magnesium. For this, we investigated its potential to chelate the magnesium by measuring its UV spectra in the absence and in the presence of magnesium ions. Results showed that **A15** maximum of absorbance did not shift in the presence of 6 mM $MgCl_2$, excluding the involvement of chelation in the mechanism of action (Figure S2). Secondly, since previous studies showed that molecules targeting the RT heterodimer dimerization could inhibit both RT-associated enzymatic activities (Tintori et al. 2016), we examined by differential scanning fluorimetry whether **A15** could alter the HIV-1 RT thermal stability (Cummings, Farnum and Nelen 2006). Results showed that **A15** did not affect RT thermal stability, differently from the positive controls used, i.e. the active site metal chelating beta-thujaplicinol (BTP), that has been shown to stabilize the RT against thermal denaturation (Su et al. 2010), and the allosteric RNase H inhibitor 2-(3,4-dihydroxyphenyl)-5,6-dimethylthieno[2,3-d]pyrimidin-4(3H)-one (VU) that has been shown to destabilize the HIV-1 RT (Masaoka et al. 2013) (Fig. 2). Of note, **A15** showed an RT thermal stability pattern similar to the one previously reported for the NNRTI efavirenz (EFV) and RMNC6 (Corona *et al.* 2016a), hence suggesting an allosteric mode of action (Figure 2).

*2.3 **A15** derivative docking studies*

To further investigate the RT−**A15** interactions, we then carried out QM polarized (QMPL) blind docking experiments. QMPL docking workflow combines docking with *ab initio* methods for ligand charges calculation within the protein environment (Schrödinger). Subsequently, the best poses were subjected to post-docking minimization to consider induced-fit protein conformation

change (that takes place after ligand binding) and implicit water solvation (Mohamadi *et al.* 1990). These studies suggested that **A15** could be able to bind into two RT pockets: one close to the polymerase catalytic site (pocket 1) and one close to RNase H catalytic site (pocket 2). According to previous reports (Himmel *et al.* 2006), **A15** binding into the first pocket could affect both RDDP and RNase H activities, the first by restricting RT thumb domain flexibility and impeding correct nucleic acid positioning, the latter by deviating the trajectory of the nucleic acid which could not be properly positioned within the RNase H active site. In agreement with this binding model, docking results showed that **A15** could occupy the area between the polymerase catalytic site and the NNRTI binding pocket (Figure 3a, 3b). Of note, the **A15**-RT complex seems to be stabilized by hydrogen bonds with D186, K223 and by π–π interaction with W229, which are important and conserved residues that are prime target for the rational design of NNRTIs (Pelemans *et al.* 2000). **A15** binding was also proposed to be stabilized by van der Waals interactions with other RT residues such as L100, V108, V111, Y188, F227 and L234. Some of these residues are included in the so called "primer grip" which plays a key role in directing the movement of RT along the template-primer. To confirm the proposed binding mode, further molecular docking studies were performed using single point mutated V108A RT (Figure 3c, 3d). Results showed that when docked with V108A RT, **A15** changed its binding mode, as compared to the wt RT complex, entering more deeply within pocket 1 cavity since steric hindrance of Alanine is lower than Valine. As also previously proposed for other dual RT inhibitors derivatives BHMP07 (Felts *et al.* 2011) and RMNC6(Felts *et al.* 2011; Corona *et al.* 2016a), blind docking experiments showed that **A15** could also bind to a second pocket (pocket 2), located below the RNase H catalytic site (Figure 4a, 4b). To confirm this hypothesized binding model, *in silico* long energy minimization studies were performed using single point mutated A502F RT. Of note, residue A502 is located in the alpha helix close to the putative binding pocket and has been reported to have a critical role also in the binding of other dual inhibitors (Corona *et al.* 2016a). Substitution of Ala with Phe caused a movement of alpha helix that reduced the space between the two subunits p51 and p66, hindering the entrance of the compound (Figure 4c, 4d). Docking experiments performed on A502F RT showed that **A15** was not able to bind into the cavity between the two subunits, mostly lying in the enzyme surface exposed to the solvent. The complex A502F RT-**A15** was hence overall less stable than the complex wt RT-**A15**.

*2.4 **A15** derivative effects on mutated RTs*

In order to confirm the hypotheses suggested by the *in silico* studies and to compare the mode of action of **A15** with the one of classical NNRTIs, site directed mutagenesis were performed independently introducing the amino acid substitutions V108A, K103N, Y181C and Y188L. In addition, also mutated A502F RT was obtained. Derivative **A15** was tested on both RNase H and

RDDP activities of these mutated RTs (Table 4). Results showed that **A15** retained a good potency of inhibition against all the three NNRTI resistant enzymes, confirming a binding to RT different from NNRTIs. Furthermore, in agreement with the docking model, the V108A substitution strongly affected the **A15** potency of RT inhibition (12.6 fold for RNase H IC_{50} value and 4.7 fold for RDDP IC_{50} value, respectively). Also in agreement with the docking model, the A502F substitution caused a 9.0 fold of increase in the RNase H IC_{50} value respect to wt RT.

Overall, we described the identification of the of 1H-pyrrole-3-carbothioamide derived scaffold as a promising starting point for the synthesis of dual RT inhibitors, identifying the 3,5-diamino-N-benzoyl-1H-pyrazole-4-(4-chloro-phenyl)carbothioamide derivative, compound **A15**, as an efficient RT and viral replication inhibitor. Mode of action studies showed that **A15** acts through a dual RT inhibition, achieved by binding to two different sites on the RT, and retained activity against enzymes carrying mutations commonly conferring resistance to NNRTIs, hence showing a potential for **A15** as a hit compound whose scaffold improvement would allow to develop new RT dual inhibitors more active against viral replication and possibly against selected NNRTI resistant viruses and less susceptible to the selection of drug resistant viruses.

3. Materials and methods

3.1 Synthesis and characterization

Compounds were synthesized by slight modification of our previously reported procedure (Cocco, et al 1995,1999, 2003, 2006) (S3. Scheme 1 and Scheme 2).

Commercially available solvents and reagents were used without further purification unless otherwise stated. ^{1}H NMR spectra were recorded on a Varian Inova 500 spectrometer. The chemical shifts (δ) are reported in part per million downfield from tetramethylsilane (TMS), which was used as internal standard, and the spectra were recorded in DMSO-d_6. Splitting patterns are designated as singlet (s), doublet (d), triplet (t), quartet (q), and multiplet (m). Infrared spectra were recorded on a Bruker Vector 22 spectrometer. The main bands are given in cm^{-1}. Melting points (m.p.) were determined on a Stuart Scientific Melting point SMP1 apparatus and are uncorrected. The purity of tested compounds was determined by combustion elemental analyses conducted by the Microanalytical Laboratory of the Chemistry Department of the University of Ferrara with a Yanagimoto MT-5 CHN recorder elemental analyzer and all values were within 0.4% of the calculated values, which indicates >95% purity of the tested compounds. Analytical thin layer chromatography was performed using 0.25 mm silica gel 60-F plates.

Cyanoacetamidrazones **10, 12, 13, 15-17** (Cocco *et al.* 1996) Pyrazoles **A1** and **A18** (Cocco *et al.* 2006), Pyrazoles **A2, A9, A14-17**(Cocco *et al.* 1999) Pyrrolecarbothioamides **B7, B18-19** (Cocco, Congiu and Onnis 1995) Pyrrolecarbothioamides **B2-3, B5-10, B12-16** (Cocco *et al.*2003) were

prepared as previously reported. The preparation and characterization of all the other pyrazole and pyrrole derivatives is described supplementary material (S4)

3.2 Biological activity

3.2.1 Expression and purification of recombinant HIV-1 RTs group M subtype B

p6HRT-prot vector was kindly provided by Dr. Stuart Le Grice Laboratory. Heterodimeric RT was expressed essentially as described (Corona *et al.* 2016a). Briefly, *E. coli* strain M15 containing the p6HRT-prot vector were grown up to an OD600 of 0.7 and induced with isopropyl β-D-1-thiogalactopyranoside (IPTG) 1.7 mM for 4 h. Cell pellets were resuspended in Lysis buffer (50 mM Sodium Phosphate pH 7.8, 0.5 mg/mL lysozyme), incubated on ice for 20 min, added 0.3 M final NaCl, sonicated and centrifuged at 30,000×g for 1 h. The supernatant was loaded into a Ni^{2+}-sepharose column pre-equilibrated with Loading Buffer (50 mM Sodium Phosphate pH 7.8, 0.3 M NaCl, 10% glycerol, 10 mM imidazole) and washed thoroughly with Wash Buffer (50 mM Sodium Phosphate pH 6.0, 0.3 M NaCl, 10% glycerol, 80 mM imidazole). RT was gradient-eluted with Elute Buffer (Wash buffer with 0.5 M imidazole). Fractions were collected, protein purity was checked by SDS-PAGE and found to be higher than 90%. RT containing fractions were pooled and diluted 1:1 with Dilute Buffer (50 mM Sodium Phosphate pH 7.0, 10% glycerol) then loaded into a Hi-trap Heparine HP GE (Healthcare Lifescience) pre-equilibrated with 10 columns volume of Loading Buffer 2 (50 mM Sodium Phosphate pH 7.0, 10% glycerol, 150 mM NaCl). Column was then washed with Loading Buffer 2 and RT was gradient-eluted with Elute Buffer 2 (50 mM Sodium Phosphate pH 7.0, 10% glycerol, 150 mM NaCl). Fractions were collected, protein was dialyzed and stored in Buffer containing 50 mM Tris HCl pH 7.0, 25 mM NaCl, 1mM EDTA, 50% glycerol. Catalytic activities and protein concentration were determined. Enzyme-containing fractions were pooled and aliquots were stored at −80 °C

3.2.2 Site-directed Mutagenesis

Amino acid substitutions were introduced into the p66 HIV-1 RT subunit coded in a p6HRT-prot plasmid using the QuikChange protocol (Agilent Technologies Inc., Santa Clara, CA).

3.2.3 HIV-1 DNA polymerase-independent RNase H activity determination

The wt and mutated HIV RT-associated RNase H activity was measured as described (Corona *et al.* 2014b) in 100 µL reaction volume containing 50 mM Tris HCl pH 7.8, 6 mM $MgCl_2$, 1 mM dithiothreitol (DTT), 80 mM KCl, hybrid RNA/DNA (5'-GTTTTCTTTTCCCCCCTGAC-3'-Fluorescein, 5'-CAAAAGAAAAGGGGGGACUG-3'-Dabcyl) and different amount of enzymes according to a linear range of dose-response curve: 20 ng of wt RT; 60 ng K103N; 75 ng V108A; 5 ng Y181C; 30 ng Y188L; 100ng A502F. The reaction mixture was incubated for 1 h at 37 °C, the

reaction was stopped by addition of EDTA and products were measured with a Victor 3 (Perkin) at 490/528 nm.

3.2.4 HIV-1 RNA-dependent DNA polymerase activity determination

The HIV-1 RT-associated RDDP activity was measured as described (Meleddu *et al.* 2014). Briefly in 25 µL volume containing 60 mM Tris-HCl pH 8.1, 8 mM $MgCl_2$, 60 mM KCl, 13 mM DTT, poly(A)-oligo(dT), 100 µM dTTP, and 6 ng wt RT (or 30 ng K103N RT; 19 ng V108A RT; 1,5 ng Y181CRT; 15 ng Y188L RT; 15ng A502F RT). After enzyme addition the reaction mixture was incubated for 30 min at 37 °C and enzymatic reaction was stopped by addition of EDTA. Reaction products were detected by picogreen addition and measured with a Victor 3 (Perkin) at 502/523 nm.

3.2.5 HIV replication

Drug-mediated inhibition of virus-induced cytotoxicity was assayed in MT-2 cells as described (Esposito *et al.* 2011) with minor modifications. Briefly, triplicate wells of 96-well plates containing $1x10^4$ MT-2 cells were infected with HIV-1 IIIB strain at a multiplicity of infection of 0.1. Serial dilutions of drug were added immediately after infection. Cell viability was quantified 5 days after infection with the MTT-dye reduction method.

3.2.6 Detection of protein inhibitor interactions by Differential Scanning Fluorimetry

Thermal stability assays were performed according to Nettleship et al.2008. To a LightCycler 480 96-well plate (Roche) 1 µL of 500 µM inhibitor in DMSO was added, followed by 49 µL of 300 nM HIV-1 RT in reaction buffer containing 20 mM HEPES, pH 7.5, 10 mM $MgCl_2$, 100 mM NaCl, and a 1:1000 dilution of Sypro Orange dye (Invitrogen). The mixture was heated from 30 to 90 °C in increments of 0.2 °C. Fluorescence intensity was measured using excitation and emission wavelengths of 483 and 568 nm, respectively. Changes in protein thermal stability (ΔTm) upon inhibitor binding were analyzed by using LightCycler 480 software. All assays were performed in triplicate.

3.3 **Molecular modelling**

3.3.1 Ligand preparation

The ligand was built within the Maestro platform, the geometry was optimized with Macromodel (Mohamadi *et al.* 1990) using the Merck Molecular Force Fields (MMFFs) (Halgren 1996), the GB/SA solvation model (Still *et al.* 1990), and the Polak-Ribier Coniugate Gradient (PRCG) method converging on gradient with a threshold of 0.05kJ/(molÅ).

3.3.2 Protein preparation

Starting crystal coordinates of the complex RT-RNase H inhibitor were downloaded from the Protein Data Bank (http://www.rcsb.org/) pdb accession code 3lp2 (Su *et al.* 2010). Afterward, the protein was then prepared using the Schrödinger protein preparation wizard (Schrödinger 2013): Hydrogen atoms were added to the system. Partial atomic charges were assigned according to the

Optimized Potential for Liquid Simulations (OPLS-2005) (Jorgensen *et al.* 1996) force field. Asn103 was mutated in Lys. A minimization was performed to optimize hydrogen atoms and to remove any high-energy contacts or distorted bonds, angles, and dihedrals. Starting from wt protein the mutated enzymes V108A-RT and A502F-RT were generated. Both mutated RTs were minimized considering OPLS force field in GB/SA implicit water (Still *et al.* 1990), setting 10000 steps interactions analysis with Polak-Ribier Coniugate Gradient (PRCG) method and a convergence criterion of 0.1 kcal/mol.

3.3.3 Docking and post-docking

Compound **A15** was docked into wt and mutated RTs applying QM-polarized ligand docking protocol applying default settings (Schrödinger). The enzyme was divided into boxes of the same size (46x46x46 Å) covering overall the whole p66 subunit. The docking grids were defined by centering on W229 and Q500. In order to better take into account the induced fit phenomena, the most energy favored generated complexes were fully optimized with the OPLS force field in GB/SA implicit water (Still *et al.* 1990), setting 10000 steps interactions analysis with Polak-Ribier Coniugate Gradient (PRCG) method and a convergence criterion of 0.1 kcal/(molÅ). The resulting complexes were considered for the binding modes graphical analysis with Pymol (Schrödinger) and Maestro (Schrödinger 2013).

Disclosure statement

No potential conflict of interest was reported by the authors.

Acknowledgements

AC, FE and ET thank Italian MIUR for financial support (PRIN 2010, 2010W2KM5L_003) and the National Foundation for Cancer Research grant number PO1CA154295.

References

Almerico AM, Mingoia F, Diana P *et al.* Pyrrolo[1,2-f]phenanthridines and related non-rigid analogues as antiviral agents. *Eur J Med Chem* 2002;**37**:3–10.

Antonucci T, Warmus JS, Hodges JC *et al.* Characterization of the antiviral activity of highly substituted pyrroles: a novel class of non-nucleoside HIV-1 reverse transcriptase inhibitor. *Antivir Chem Chemother* 1995;**6**:98–108.

Billamboz M, Bailly F, Barreca ML *et al.* Design, Synthesis, and Biological Evaluation of a Series of 2-Hydroxyisoquinoline-1,3(2H,4H)-diones as Dual Inhibitors of Human Immunodeficiency Virus Type 1 Integrase and the Reverse Transcriptase RNase H Domain Muriel. *J Med Chem* 2008;**3**:7717–30.

Billamboz M, Bailly F, Lion C *et al.* Magnesium Chelating 2-Hydroxyisoquinoline-1,3 (2H, 4H)-dionese as Inhibitors of HIV-1 Integrase and / or the HIV-1 Reverse Transcriptase

Ribonuclease H Domain : Discovery of a Novel Selective Inhibitor of the Ribonuclease H Function. *J Med Chem* 2010;**3**:1812–24.

Carcelli M, Rogolino D, Gatti A *et al.* Chelation Motifs Affecting Metal-dependent Viral Enzymes : N -acylhydrazone Ligands as Dual Target Inhibitors of HIV-1 Integrase and Reverse Transcriptase Ribonuclease H Domain. 2017;**8**:1–10.

Chung S, Himmel DM, Jiang J-K *et al.* Synthesis, activity, and structural analysis of novel α-hydroxytropolone inhibitors of human immunodeficiency virus reverse transcriptase-associated ribonuclease H. *J Med Chem* 2011;**54**:4462–73.

Cocco MT, Congiu C, Lilliu V *et al.* Amidrazones as Precursors of Biologically Active Compounds - Synthesis of Diaminopyrazoles for Evaluation of Anticancer Activity. *Arch Pharm (Weinheim)* 2006;**339**:7–13.

Cocco MT, Congiu C, Onnis V. Propenethioamides in the synthesis of heterocyclic systems. Synthesis of pyrrole and 1,4-thiazepine derivatives. *J Heterocycl Chem* 1995;**32**:1679–82.

Cocco MT, Congiu C, Onnis V *et al.* New Trifluoromethylated Pyridines from Functionalized N1-Acylacetamidrazones. *J Heterocycl Chem* 1996;**33**:1771–3.

Cocco MT, Congiu C, Onnis V *et al.* A facile synthesis of 3,5-diaminopyrazole-4-carbothioamides and 3,5-diaminopyrazole-4-carboxylates. *J Heterocycl Chem* 1999;**36**:1183–8.

Cocco MT, Congiu C, Onnis V. Synthesis and In Vitro Antitumoral Activity of New N -Phenyl-3-pyrrolecarbothioamides. *Bioorg Med Chem* 2003;**11**:495–503.

Cohen MS, Hellmann N, Levy JA *et al.* The spread, treatment, and prevention of HIV-1: evolution of a global pandemic. *J Clin Invest* 2008;**118**:1244–54.

Corbau R, Mori J, Phillips C *et al.* Lersivirine, a nonnucleoside reverse transcriptase inhibitor with activity against drug-resistant human immunodeficiency virus type 1. *Antimicrob Agents Chemother* 2010;**54**:4451–63.

Corona A, Esposito F, Tramontano E. Can the ever-promising target HIV reverse transcriptase-associated RNase H become a success story for drug development? *Future Virol* 2014;**9**:445–8.

Corona A, Di Leva FS, Thierry S *et al.* Identification of Highly Conserved Residues Involved in Inhibition of HIV-1 RNase H Function by Diketo Acid Derivatives. *Antimicrob Agents Chemother* 2014a;**58**:6101–10.

Corona A, Masaoka T, Tocco G *et al.* Active site and allosteric inhibitors of the ribonuclease H activity of HIV reverse transcriptase. *Futur Med Chem* 2013;**5**:2127–39.

Corona A, Meleddu R, Esposito F *et al.* Ribonuclease H/DNA Polymerase HIV-1 Reverse Transcriptase Dual Inhibitor: Mechanistic Studies on the Allosteric Mode of Action of Isatin-Based Compound RMNC6. *PLoS One* 2016a;**11**:e0147225.

Corona A, Saverio F, Rigogliuso G *et al.* New insights into the interaction between pyrrolyl diketoacids and HIV-1 integrase active site and comparison with RNase H. *Antiviral Res* 2016b;**134**:236–43.

Corona A, Schneider A, Schweimer K *et al.* Inhibition of foamy virus reverse transcriptase by human immunodeficiency virus type 1 ribonuclease H inhibitors. *Antimicrob Agents Chemother* 2014b;**58**:4086–93.

Costi R, Métifiot M, Chung S *et al.* Basic Quinolinonyl Diketo Acid Derivatives as Inhibitors of HIV Integrase and their Activity against RNase H Function of Reverse Transcriptase. *J Med Chem* 2014:3223–34.

Cox BD, Prosser AR, Sun Y *et al.* Pyrazolo-Piperidines Exhibit Dual Inhibition of CCR5/CXCR4 HIV Entry and Reverse Transcriptase. *ACS Med Chem Lett* 2015;**6**:753–7.

Cummings MD, Farnum M a, Nelen MI. Universal screening methods and applications of ThermoFluor. *J Biomol Screen* 2006;**11**:854–63.

Cuzzucoli Crucitti G, Métifiot M, Pescatori L *et al.* Structure-Activity Relationship of Pyrrolyl Diketo Acid Derivatives as Dual Inhibitors of HIV-1 Integrase and Reverse Transcriptase Ribonuclease H Domain. *J Med Chem* 2015;**58**:1915–28.

Ding J, Das K, Moereels H *et al.* Structure of HIV-1 RT/TIBO R 86183 complex reveals similarity in the binding of diverse nonnucleoside inhibitors. *Nat Struct Biol* 1995;**2**:407–15.

Distinto S, Maccioni E, Meleddu R *et al.* Molecular Aspects of the RT/drug Interactions. Perspective of Dual Inhibitors. *Curr Pharm Des* 2013;**19**:1850–9.

Esposito F, Kharlamova T, Distinto S *et al.* Alizarine derivatives as new dual inhibitors of the HIV-1 reverse transcriptase-associated DNA polymerase and RNase H activities effective also on the RNase H activity of non-nucleoside resistant reverse transcriptases. *FEBS J* 2011;**278**:1444–57.

Felts AK, Labarge K, Bauman JD *et al.* Identification of alternative binding sites for inhibitors of HIV-1 ribonuclease H through comparative analysis of virtual enrichment studies. *J Chem Inf Model* 2011;**51**:1986–98.

Gregson J, Tang M, Ndembi N *et al.* Global epidemiology of drug resistance after failure of WHO recommended first-line regimens for adult HIV-1 infection: A multicentre retrospective cohort study. *Lancet Infect Dis* 2016;**16**:565–75.

Halgren TA. Merck molecular force field. II. MMFF94 van der Waals and electrostatic parameters for intermolecular interactions. *J Comput Chem* 1996;**17**:520–52.

Himmel DM, Sarafianos SG, Dharmasena S *et al.* HIV-1 reverse transcriptase structure with RNase H inhibitor dihydroxy benzoyl naphthyl hydrazone bound at a novel site. *ACS Chem Biol* 2006;**1**:702–12.

Jorgensen WL, Jorgensen WL, Maxwell DS *et al.* Development and Testing of the OLPS All-Atom Force Field on Conformational Energetics and Properties of Organic Liquids. *J Am Chem Soc* 1996;**118**:11225–36.

Kankanala J, Kirby KA, Liu F *et al.* Design, Synthesis, and Biological Evaluations of Hydroxypyridonecarboxylic Acids as Inhibitors of HIV Reverse Transcriptase Associated RNase H. *J Med Chem* 2016;**59**:5051–62.

Kim BS, Park JA, Kim M-J *et al.* Identification of a novel type of small molecule inhibitor against HIV-1. *BMB Rep* 2015;**48**:121–6.

Klumpp K, Mirzadegan T. Recent progress in the design of small molecule inhibitors of HIV RNase H. *Curr Pharm Des* 2006;**12**:1909–22.

Kumar S, Vernekar V, Tang J *et al.* Double-winged 3-Hydroxypyrimidine-2,4-diones: Potent and Selective Inhibition against HIV-1 RNase H with Significant Antiviral Activity. 2017a.

Kumar S, Vernekar V, Tang J *et al.* Double-winged 3-Hydroxypyrimidine-2,4-diones: Potent and Selective Inhibition against HIV-1 RNase H with Significant Antiviral Activity. *J Med Chem* 2017b:acs.jmedchem.7b00440.

Liu G-N, Luo R-H, Zhou Y *et al.* Synthesis and Anti-HIV-1 Activity Evaluation for Novel 3a,6a-Dihydro-1H-pyrrolo[3,4-c]pyrazole-4,6-dione Derivatives. *Molecules* 2016;**21**:1198.

Mao C, Vig R, Venkatachalam TK *et al.* Structure-based design of N-[2-(1-piperidinylethyl)]-N'-[2-(5-bromopyridyl)]-thiourea and N-[2-(1-piperazinylethyl)]-N'-[2-(5-bromopyridyl)]-thiourea as potent non-nucleoside inhibitors of HIV-1 reverse transcriptase. *Bioorg Med Chem Lett* 1998;**8**:2213–8.

Masaoka T, Chung S, Caboni P *et al.* Exploiting Drug-Resistant Enzymes as Tools To Identify Thienopyrimidinone Inhibitors of Human Immunodeficiency Virus Reverse Transcriptase-Associated Ribonuclease H. *J Med Chem* 2013;**56**:5436–45.

Meleddu R, Cannas V, Distinto S *et al.* Design, synthesis, and biological evaluation of 1,3-diarylpropenones as dual inhibitors of HIV-1 reverse transcriptase. *ChemMedChem* 2014;**9**:1869–79.

Meleddu R, Distinto S, Corona A *et al.* (3Z)-3-(2-[4-(aryl)-1,3-thiazol-2-yl]hydrazin-1-ylidene)-2,3-dihydro-1H-indol-2-one derivatives as dual inhibitors of HIV-1 reverse transcriptase. *Eur J Med Chem* 2015;**93**:452–60.

Menéndez-Arias L, Sebastián-Martín A, Álvarez M. Viral reverse transcriptases. *Virus Res* 2016, DOI: 10.1016/j.virusres.2016.12.019.

Mohamadi F, RIchards NGJ, Giuda WC *et al.* Macromodel—an integrated software system for modeling organic and bioorganic molecules using molecular mechanics. *J Comput Chem* 1990;**11**:440–67.

Mowbray CE, Burt C, Corbau R *et al.* Pyrazole NNRTIs 1: Design and initial optimisation of a novel template. *Bioorganic Med Chem Lett* 2009;**19**:5599–602.

Patel R V., Park SW. Pyrroloaryls and pyrroloheteroaryls: Inhibitors of the HIV fusion/attachment, reverse transcriptase and integrase. *Bioorg Med Chem* 2015;**23**:5247–63.

Pelemans H, Esnouf R, De Clercq E *et al.* Mutational analysis of trp-229 of human immunodeficiency virus type 1 reverse transcriptase (RT) identifies this amino acid residue as a prime target for the rational design of new non-nucleoside RT inhibitors. *Mol Pharmacol* 2000;**57**:954–60.

Schatz O, Cromme F, Naas T *et al.* Inactivation of the RNase H domain of HIV-1 reverse transcriptase blocks viral infectivity. *Gene Regul AIDS* 1990:293–404.

Schrödinger L. QMPolarized protocol.

Schrödinger L. PyMOL,Molecular Graphics System.

Schrödinger L. Maestro GUI. 2013.

Still WC, Tempczyk A, Hawley RC *et al.* Semianalytical treatment of solvation for molecular mechanics and dynamics. *J Am Chem Soc* 1990;**112**:6127–6129.

Su H-P, Yan Y, Prasad GS *et al.* Structural basis for the inhibition of RNase H activity of HIV-1 reverse transcriptase by RNase H active site-directed inhibitors. *J Virol* 2010;**84**:7625–33.

Tang J, Maddali K, Dreis CD *et al.* 6-Benzoyl-3-hydroxypyrimidine-2,4-diones as dual inhibitors of HIV reverse transcriptase and integrase. *Bioorg Med Chem Lett* 2011;**21**:2400–2.

Tang J, Vernekar SK V, Chen Y-L *et al.* Synthesis, biological evaluation and molecular modeling of 2-Hydroxyisoquinoline-1,3-dione analogues as inhibitors of HIV reverse transcriptase associated ribonuclease H and polymerase. *Eur J Med Chem* 2017;**133**:85–96.

Tintori AC, Corona A, Esposito F *et al.* Inhibition of HIV-1 Reverse Transcriptase Dimerization by Small Molecules. *ChemBioChem* 2016:683–8.

Tramontano E, Esposito F, Badas R *et al.* 6-[1-(4-Fluorophenyl)methyl-1H-pyrrol-2-yl)]-2,4-dioxo-5-hexenoic acid ethyl ester a novel diketo acid derivative which selectively inhibits the HIV-1 viral replication in cell culture and the ribonuclease H activity in vitro. *Antiviral Res* 2005;**65**:117–24.

Wang X, Gao P, Menéndez-Arias L *et al.* Update on Recent Developments in Small Molecular HIV-1 RNase H Inhibitors (2013-2016): Opportunities and Challenges. *Curr Med Chem* 2017.

Wildum S, Paulsen D, Thede K *et al.* In Vitro and In Vivo Activities of AIC292, a Novel HIV-1 Nonnucleoside Reverse Transcriptase Inhibitor. *Antimicrob Agents Chemother* 2013;**57**:5320–9.

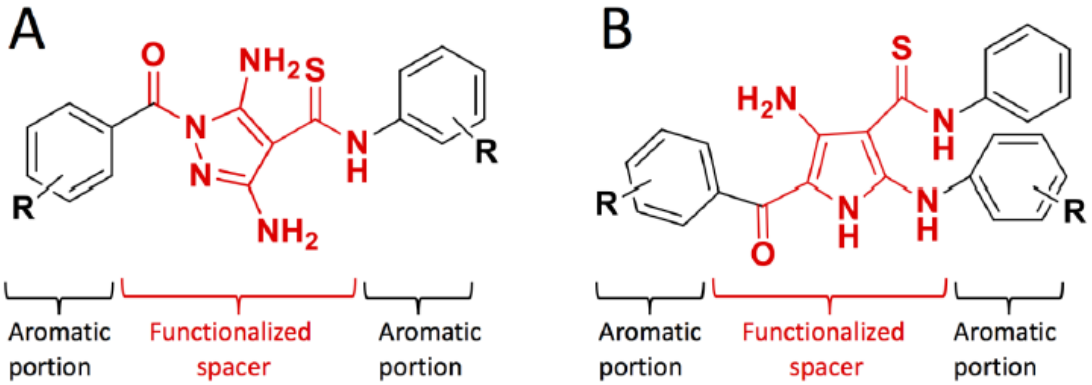

Figure 1. Schematic representation of synthesized compounds: Panel A: 3,5-diamino-N-aryl-1*H*-pyrazole-4-carbothioamide derivatives. **Panel B:** 4-amino-5-benzoyl-N-phenyl-2-(substituted-amino)-1*H*-pyrrole-3-carbothioamide derivatives.

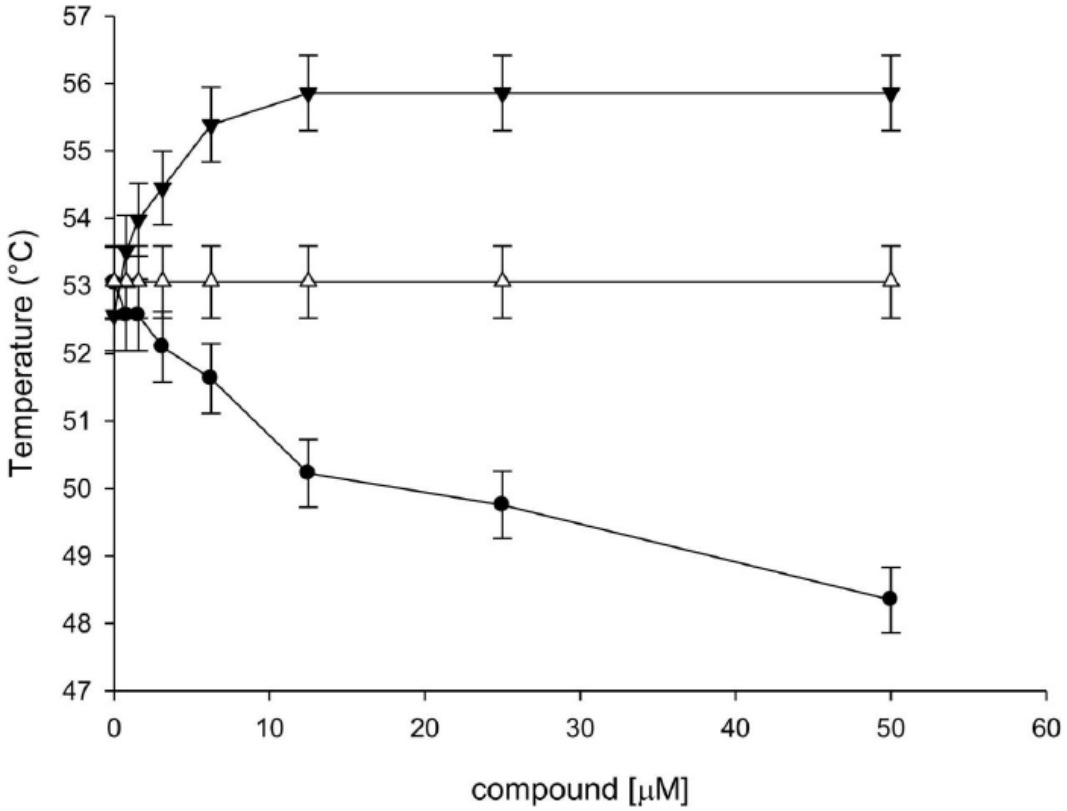

Figure 2. Effect of A15 on the thermal stability of p66/p51 HIV-1 RT. The melting temperature of HIV-1 RT was measured by differential scanning fluorimetry in presence of increasing concentrations of (▼) BTP, (●) VU and (Δ) **A15.**

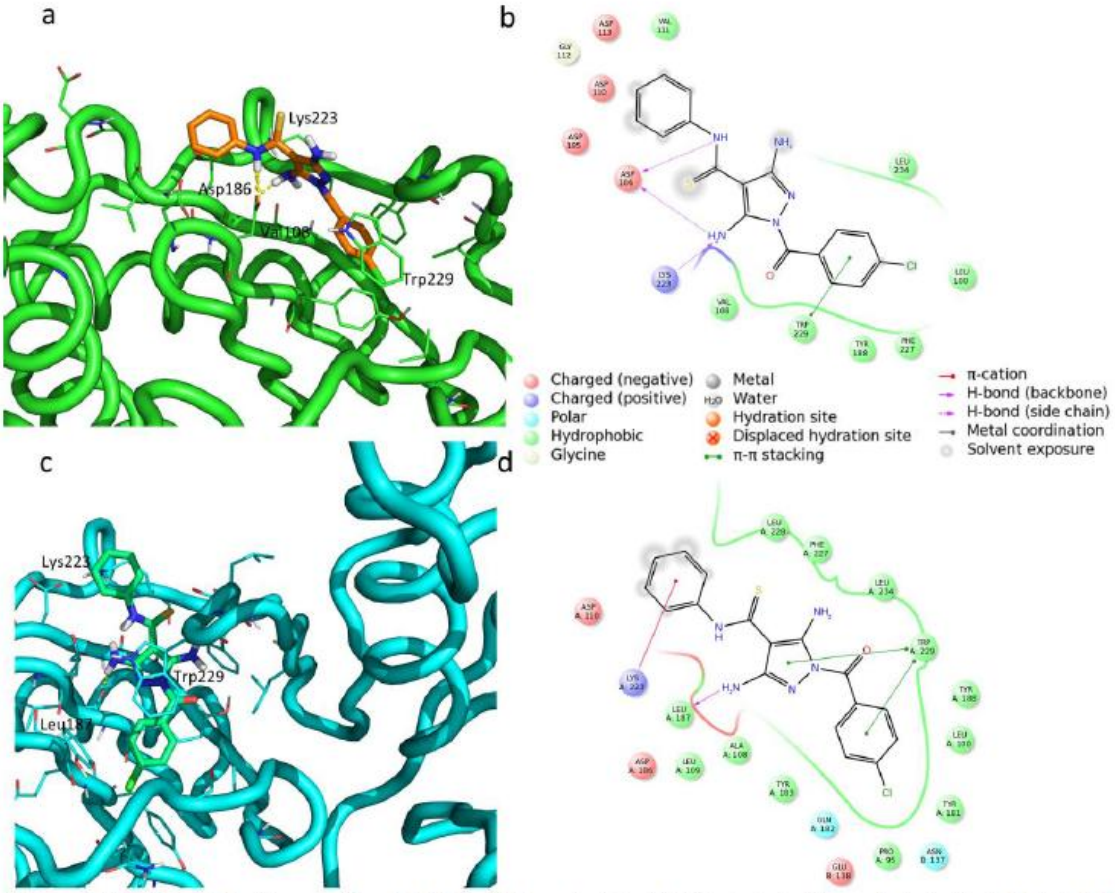

Figure 3. Putative binding mode of A15 in RT pocket 1. a) **A15** depicted in pocket 1 of wt-RT; c) **A15** depicted in pocket 1 in complex of RT-V108A; b-d) 2D representation of **A15** in complex with wt and V108A RT, respectively, with indication of binding pocket interacting residues.

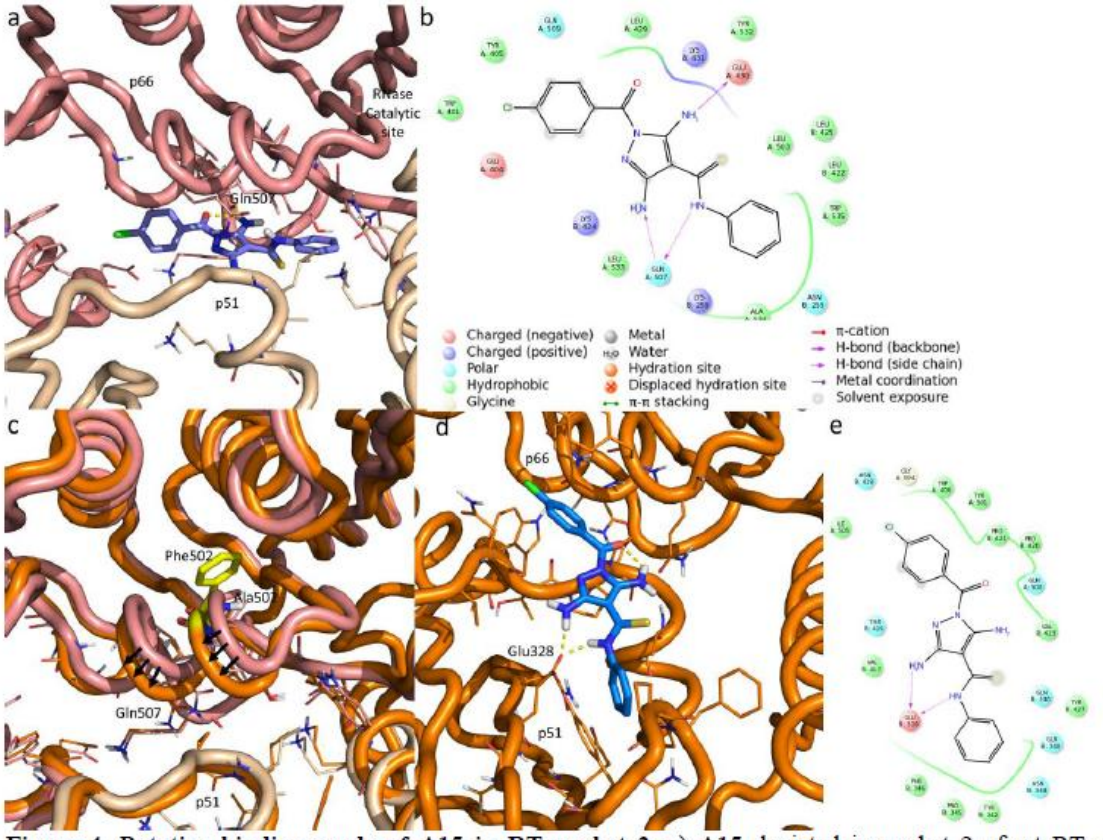

Figure 4. Putative binding mode of A15 in RT pocket 2. a) **A15** depicted in pocket 2 of wt RT; c) conformational change of the pocket 2 upon mutation of A502F RT (in yellow); wt RT is colored in pink and the A502F RT in orange, residues interacting with the compound are in sticks; d) **A15** depicted A15 in RT-A502F pocket 2; b-e) 2D representation of **A15** in complex with wt and A502F RT, respectively, with indication of binding pocket interacting residues.

Table1. HIV-1 RT-associated RNase H inhibition by 3,5-diaminopyrazole derivatives.

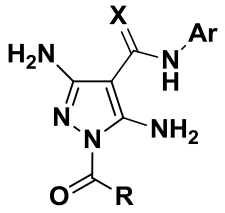

Comp.	X	Ar	R	RNase H [a]IC_{50} (µM)
A1	S	C_6H_5	C_6H_5	98 ± 8
A2	S	C_6H_5	$C_6H_5CH_2$	19 ± 3
A3	S	C_6H_5	4-$OCH_3C_6H_4CH_2$	> 100
A4	S	C_6H_5	4-$NO_2C_6H_4CH_2$	> 100
A5	S	C_6H_5	4-$ClC_6H_4CH_2$	4.0 ± 0.9
A6	O	C_6H_5	4-$ClC_6H_4CH_2$	5.0 ± 1.2
A7	S	C_6H_5	2,4-$Cl_2C_6H_3CH_2$	> 100
A8	S	3-ClC_6H_4	4-$ClC_6H_4CH_2$	> 100
A9	S	4-ClC_6H_4	4-$ClC_6H_4CH_2$	> 100
A10	S	4-F C_6H_4	4-$ClC_6H_4CH_2$	> 100
A11	S	2,4-ClC_6H_3	4-$ClC_6H_4CH_2$	> 100
A12	S	3,4-ClC_6H_3	4-$ClC_6H_4CH_2$	> 100
A13	S	2,5-ClC_6H_3	4-$ClC_6H_4CH_2$	21 ± 5
A14	S	4-$OCH_3C_6H_4$	4-$ClC_6H_4CH_2$	> 100
A15	S	4-ClC_6H_4	C_6H_5	7.0 ± 2.0
A16	S	4-ClC_6H_4	$C_6H_5CH_2$	> 100
A17	S	*i*-C_3H_7	C_6H_5	> 100
A18	O	*i*-C_3H_7	C_6H_5	48 ± 6

[a]Compound concentration (± standard deviation) required to reduce the HIV-1 RT-associated RNase H activity by 50%.

Table 2. HIV-1 RT-associated RNase H inhibition by 4-amino-1*H*-pyrrole-3-carbothioamide derivatives.

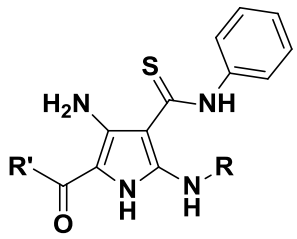

Compd.	R	R'	RNase H [a]IC_{50} (μM)
B1	4-$CH_3C_6H_4$	C_6H_5	6.1 ± 1.6
B2	4-$CH_3C_6H_4$	4-$CH_3C_6H_4$	8.2 ± 1.7
B3	4-$CH_3C_6H_4$	4-$OCH_3C_6H_4$	8.0 ± 2.6
B4	4-$CH_3C_6H_4$	4-ClC_6H_4	> 100
B5	4-$CH_3C_6H_4$	4-BrC_6H_4	8.3 ± 2.0
B6	4-$CH_3C_6H_4$	3,4-$Cl_2C_6H_3$	> 100
B7	4-$OCH_3C_6H_4$	CH_3	> 100
B8	4-$OCH_3C_6H_4$	C_6H_5	19 ± 3
B9	4-$OCH_3C_6H_4$	4-$CH_3C_6H_4$	> 100
B10	4-$OCH_3C_6H_4$	4-$OCH_3C_6H_4$	> 100
B11	4-$OCH_3C_6H_4$	4-BrC_6H_4	> 100
B12	4-$OCH_3C_6H_4$	4-ClC_6H_4	> 100
B13	4-$OCH_3C_6H_4$	3,4-$Cl_2C_6H_3$	> 100
B14	4-ClC_6H_4	C_6H_5	20 ± 4
B15	4-ClC_6H_4	4-$CH_3C_6H_4$	9.0 ± 2.0
B16	4-ClC_6H_4	4-$OCH_3C_6H_4$	8.0 ± 2.1
B17	4-ClC_6H_4	4-ClC_6H_4	8.2 ± 2.4
B18	*i*-C_3H_7	C_6H_5	> 100
B19	$C_6H_5CH_2$	C_6H_5	18 ± 3
B20	4-OCH_3-2-pyridyl	C_6H_5	> 100

[a]Compound concentration (± standard deviation) required to reduce the HIV-1 RT-associated RNase H activity by 50%

Table 3. Inhibition of HIV-1 replication inhibition by selected 3,5-diaminopyrazole and 4-amino-1*H*-pyrrole-3-carbothioamide derivatives.

	HIV-1 [a]EC_{50} (μM)	[b]CC_{50} (μM)	
Compounds		**TZMbl**	**CEM cells**
A2	> 50	> 50 (100%)[c]	> 50 (98%)[c]
A5	> 50	> 50 (100%)[c]	> 50 (94%)[c]
A6	> 50	> 50 (100%)[c]	> 50 (92%)[c]
A15	25 ± 2	44 ± 3	> 50 (79%)[c]
B1	> 30	30 ± 5	> 50 (85%)[c]
B2	> 6.7	6.7 ± 1.2	11 ± 2
B3	> 8.7	8.7 ± 1.4	7.5 ± 0.6
B5	> 30	9.0 ± 1.8	> 50 (57%)[c]
B8	> 30	8.5 ± 1.3	50 ± 2
B14	> 30	30 ± 4	> 50 (80%)[c]
B15	> 30	30 ± 2	54 ± 3
B16	> 25	25 ± 3	36 ± 5
B17	> 18	18± 2	24 ± 3
B19	> 7.2	7.2 ± 0.6	13 ± 2
EFV	0.14 ± 0.02	> 50 (100%)[c]	> 50 (100%)[c]

[a]Compound concentration (± standard deviation) required to decrease viral replication in TZMbl cells by 50%

[b]Compound concentration (± standard deviation) required to reduce cell viability by 50%.

[c]Percentage of cells viability in presence of 50 μM inhibitor

Table 4. Inhibition of HIV-1 mutated RT-associated RNase H and RDDP activities by A15.

	A15				BTP			Efavirenz	
	RNase H		RDDP		RNase H			RDDP	
RT	IC_{50} (μM)[a]	fold	IC_{50} (μM)[b]	fold	IC_{50} (μM)[a]	fold		IC_{50} (nM)[b]	fold
wt	7.7 ± 2.0	1	17 ± 4	1	0.19 ± 0.03	1		23 ± 4	1
K103N	22 ± 4	2.9	37 ± 2	2.2	0.22 ± 0.08	1.2		176 ± 25	7.6
Y181C	28 ± 1	3.6	32 ± 3	1.9	0.23 ± 0.05	1.2		50 ± 9	2.2
Y188L	14 ± 1	1.8	32 ± 2	1.9	0.08 ± 0.05	0.4		198 ± 60	8.6
V108A	96 ± 18	12.6	82 ± 2	4.8	0.18 ± 0.04	0.9		21 ± 3	0.9
A502F	69 ± 14	9.0	24 ± 3	1.4	0.17 ± 0.03	0.9		25 ± 2	1.1

[a]Compound concentration (± standard deviation) required to inhibit HIV-1 RT-associated RNase H activity by 50%.
[b]Compound concentration (± standard deviation) required to inhibit HIV-1 RT-associated RDDP activity by 50%.